

Figure 11: The phase diagram for system (16) with the inhomogeneity in the natural frequency in the parameter space $(\tilde{\sigma} = \sigma/\lambda, \tilde{\mu} = \mu/\lambda)$: a zoom-in of the region surrounding the tip of the region where three equilibria of ODE (22), one asymptotically stable exist. The region containing two asymptotically stable equilibria and one unstable equilibrium is shaded pink. The area with one asymptotically stable equilibrium and two unstable is shaded green. The areas where the unique equilibrium is asymptotically stable or unstable are yellow and blue, respectively.

A proof of Proposition 1 is found in Appendix B. Here, we make a few remarks.

- Remark.**
1. The blow up of $|v|$ as $\tilde{\mu}^{-1/3}$ at $\tilde{\sigma} = 0$ as $\tilde{\mu} \rightarrow 0$ is consistent with the result proven in [23]. Indeed, recalling that $\tilde{\mu} = \mu/\lambda$ and $z_2 = \sqrt{\mu}e^{i\omega t}$, we obtain $|z_2| \approx \lambda^{1/3}\mu^{1/6}$ as $\mu \rightarrow 0$.
 2. If $\tilde{\sigma} \neq 0$, the amplification factor of the amplitude in the second cell is bounded from above by $\tilde{\sigma}^{-2} = \lambda^2/\sigma^2$. Hence, increasing the coupling strength and reducing frequency inhomogeneity increases the amplification effect.
 3. In the phase-locked regime, i.e., when an asymptotically stable periodic solution to ODE (16) exists, the amplitude in the second cell may be larger or smaller than the amplitude in the first cell. The ratio of the amplitudes is bounded from below by $\frac{1}{2}$, i.e., $|z_2|/|z_1| > \frac{1}{2}$. This immediately follows from the stability condition that the trace of the Jacobian of Eq. (22) must be negative – see the proof.

4.1.3 Invariant tori

Fig. 10 shows that when the natural frequency difference $|\tilde{\sigma}|$ is large enough, then the system has no periodic attractors. In this case, system (16) settles on an invariant torus attractor, so that cell z_1 performs a periodic motion with frequency ω , and cell z_2 settles onto a limit cycle in the co-rotating frame of frequency ω . If we fix $\tilde{\mu}$ and move along $\tilde{\sigma}$, the torus attractor appears as a result of a saddle-node bifurcation, if $\tilde{\mu} > \frac{4\sqrt{2}}{3} \approx 1.8856$, and as a result of a Hopf bifurcation, if $0 < \tilde{\mu} < \frac{4\sqrt{2}}{3}$. Fig. 12 illustrates the change of the direction field and the birth of the torus attractor, which corresponds to a limit cycle in the co-rotating frame, at $\tilde{\mu} = 3.0, 1.91$, and 0.5 . The invariant tori at $\lambda = 1$ and selected values of μ and σ soon after the bifurcation point are shown in Fig. 13.

4.2 Inhomogeneity in the excitation parameter and the natural frequency

In this section, we consider system (32) with inhomogeneities in the excitation parameter μ and the natural frequency ω , represented by ε and σ , respectively. The schematic of the feedforward network is shown in Fig. 14.

$$\begin{aligned} \dot{z}_1 &= (\mu + i\omega)z_1 - |z_1|^2 z_1 \\ \dot{z}_2 &= ((\mu + \varepsilon) + i(\omega + \sigma))z_2 - |z_2|^2 z_2 - \lambda z_1. \end{aligned} \quad (32)$$

Figure 14: A schematic diagram of a two-cell feed-forward network with Stuart-Landau cells with inhomogeneities in the natural frequency and the excitation parameter represented by σ and ε , respectively.

We assume that $\sigma \in \mathbb{R}$, $\mu > 0$ and $\lambda > 0$. Further, we will distinguish two cases: $\mu + \varepsilon \leq 0$ and $\mu + \varepsilon > 0$. If $\mu + \varepsilon \leq 0$, there exists a unique globally attracting periodic solution to Eq. (32). If $\mu + \varepsilon > 0$, an appropriate variable change together with a time scaling and a redefinition of parameters reduces the number of parameters to two and reduces Eq. (32) to Eq. (22) analyzed in Section 4.1.

4.2.1 The reduced system

We assume that the first cell, z_1 , is at its periodic attractor, i.e., $z_1 = \sqrt{\mu}e^{i\omega t}$. Let $z_2(t) = u(t)e^{i\omega t}$, where $u(t) \in \mathbb{C}$ is the second cell in the co-rotating frame. The ODE for u is

$$\dot{u} = (\mu + \varepsilon)u - |u|^2 u + i\sigma u - \lambda\sqrt{\mu}. \quad (33)$$

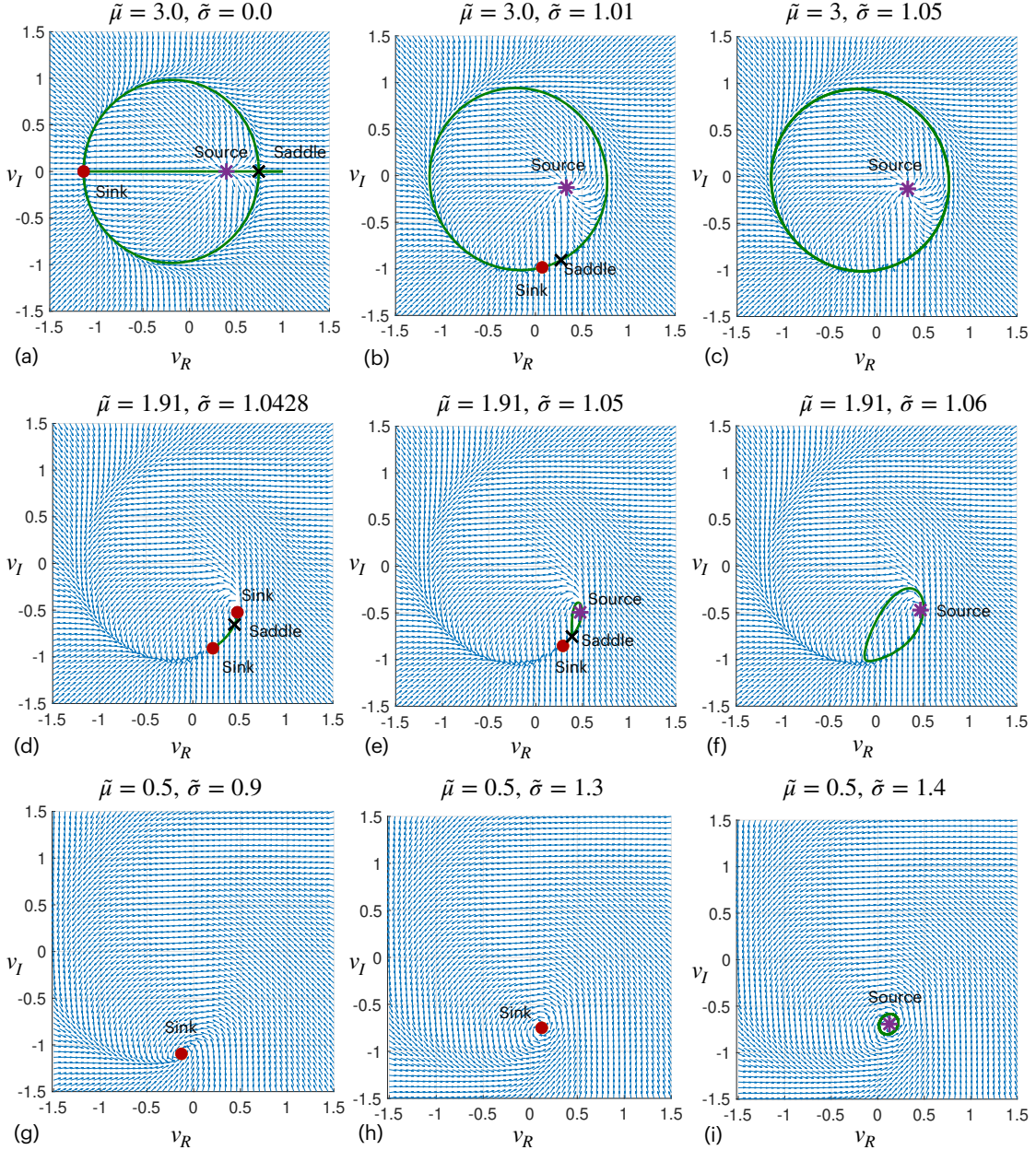


Figure 12: The direction fields of ODE (22) at selected values of $\tilde{\mu}$ and $\tilde{\sigma}$. The birth of the limit cycle of ODE (22), which corresponds to the invariant torus of ODE (16), occurs via a saddle-node bifurcation, as at $\tilde{\mu} = 3$ and 1.91, or a Hopf bifurcation, as at $\tilde{\mu} = 0.5$. The plot in (d) exemplifies a bistability situation.